Available online at www.sciencedirect.com
ScienceDirect
Journal of Catalysis 244 (2006) 33–42
JOURNAL OF CATALYSIS
www.elsevier.com/locate/jcat

# Thermally stable ion-exchange resins as catalysts for the liquid-phase dehydration of 1-pentanol to di-*n*-pentyl ether (DNPE)

Roger Bringué, Montserrat Iborra, Javier Tejero *, José Felipe Izquierdo, Fidel Cunill, Carles Fité, Victor J. Cruz

*Department of Chemical Engineering, Faculty of Chemistry, University of Barcelona, C/Martí i Franquès 1, 08028-Barcelona, Spain*

Received 27 October 2005; revised 27 March 2006; accepted 17 July 2006

Available online 28 September 2006

**Abstract**

Conversion, selectivity, yield, and kinetics of the liquid-phase dehydration of 1-pentanol to di-*n*-pentyl ether (DNPE) were determined at 403–463 K on a recently developed sulfonated resin, Amberlyst 70, which is thermally stable up to 473 K. The behavior of Amberlyst 70 was compared with that of Nafion resin NR50, an H-Beta zeolite, and styrene-divinylbenzene resins stable up to 423 K (i.e., Amberlyst 36 and CT-224). Amberlyst 70 was found to be the most suitable catalyst for this application, showing the highest conversion and yield, with a selectivity to DNPE $\geqslant 93\%$, despite the fact that NR50 showed the highest selectivity to ether at 423–463 K. The kinetic study reveals that a model stemming from an ER mechanism in which 1-pentanol from the liquid phase reacts with 1-pentanol adsorbed on a single center to give ether adsorbed on a single site represents data on each catalyst. The activation energy was computed to be in the range 110–120 kJ/mol on all the catalysts.


*Keywords:* DNPE; Amberlyst 70; Amberlyst 36; NR50; H-Beta; 1-Pentanol; Dehydration reaction; ISEC characterization of ion-exchangers

## 1. Introduction

Diesel fuel specifications are becoming increasingly stringent as legislation is adopted to improve air quality by reducing emissions. Forthcoming diesel fuels are expected to have a higher cetane number, lower density, and lower aromatic, polyaromatic, and sulfur content compared with currently available fuels. A feasible option for meeting these regulations may be the use of reformulated diesel fuels containing appropriate high-quality components [1].

A few years ago, comprehensive study on the blending properties of oxygenates in diesel fuels [2] found that linear ethers with $\geqslant 9$ carbon atoms showed the best balance among blending cetane number and cold flow properties. Di-*n*-pentyl ether (DNPE) was selected because of its blending properties and availability of potential feedstocks. DNPE has a blending cetane number of 109, and, because of its slightly lower density and viscosity compared with commercial fuels, it behaves as a light diesel fuel. Moreover, DNPE has proven very effective in reducing diesel exhaust emissions such as CO, $NO_x$, unburned hydrocarbons, particulates, and smoke [3,4].

1-butene is an appropriate feedstock for obtaining DNPE at an industrial scale. The synthesis route consists of selective hydroformylation and hydrogenation of 1-butene to 1-pentanol, followed by a bimolecular dehydration reaction of the alcohol to di-alkyl ether. If the catalyst is not selective, then monomolecular dehydration to alkene can occur [5]. Alkene can react with the remaining alcohol to form branched ethers. Therefore, if high selectivity to linear ethers is desired, then minimizing the production of alkenes is necessary.

In previous work, the liquid-phase dehydration of 1-pentanol to DNPE without water removal was studied on gel and macroporous acidic styrene-divinylbenzene (S/DVB) resins, including sulfonated and oversulfonated ones [6]. It was found that gel-type resins are suitable catalysts for the reaction, because they are very selective to DNPE. However, because the maximum operating temperature was limited to 423 K due to thermal stability considerations, reaction rates were quite low. Therefore, it is necessary to improve the thermal stability of sul-

* Corresponding author. Fax: +31 93 4021291.
*E-mail address:* jtejero@ub.edu (J. Tejero).

0021-9517/$ – see front matter 
doi:10.1016/j.jcat.2006.07.035

fonated S/DVB resins to make it possible to work at temperatures above 423 K. Consequently, the reaction rate would be sufficiently high, and the process for obtaining DNPE in industry could be economically feasible.

The need for S/DVB ion-exchange resins with increased thermal stability is clear in other industrial processes as well, such as light-olefin hydration to alcohol. That is why ion-exchanger manufacturers do research on developing acidic resins able to work at temperatures between 423 and 473 K. Recently, thermally stable resins have been obtained by halogenating the aromatic rings as well as the aliphatic polymer backbone; some of these showed <10% losses of sulfonic acid groups in hydrolytic stability tests performed at 473 K for 24 h [7].

The aim of this work is to study the liquid-phase dehydration of 1-pentanol to DNPE without water removal over a recently developed thermally stable S/DVB resin, Amberlyst 70, which can work at temperatures as high as 473 K. To assess this resin's efficiency as a catalyst for DNPE synthesis, its behavior is compared with some S/DVB resins stable up to 423 K, and other stable up to 443 K. Moreover, it was also compared with two thermally stable catalysts of very different nature: the perfluoroalkanesulfonic resin Nafion NR50 and an H-Beta zeolite. This zeolite was selected because it works very well in etherification reaction of isobutene with alcohol in both liquid and gas phases [8–12]. Kinetic studies of the dehydration of 1-pentanol to DNPE over tested catalysts were also performed.

## 2. Experimental

### 2.1. Materials

1-Pentanol (99% pure, <1% 2-methyl-1-butanol), supplied by Fluka, was used without further purification. Bidistilled water and di-*n*-pentyl ether (⩾99%), 1-pentene (⩾97%), *cis*-2-pentene (⩾98%), *trans*-2-pentene (⩾99%), and 2-methyl-1-butanol (⩾98%) were also used for analysis purposes. Tested catalysts were thermally stable resins Amberlyst DL-H/03 and DL-I/03, both experimental samples, and Amberlyst 70 (Rohm and Haas); conventional resins CT-224 (Purolite), Dowex 50W × 4 (Aldrich), and Amberlyst 36 (Rohm and Haas); the perfluoro-alkanesulfonic resin Nafion NR50 (Aldrich); and H-Beta zeolite (Südchemie). Properties and short names are given in Table 1. Resin acid capacity was measured by titration against a standard base [13].

Structural parameters of S/DVB resins both in a dry state and swollen in water are given in Table 1. Macroporous resins consist of large agglomerates of gel microspheres, each of which comprises smaller nodules that are more or less fused together [14]. In between the nodules is a family of very small pores (micropores), and in between the microspheres is a second family of intermediate pores with diameters of 8–20 nm (mesopores). A third family of large pores with diameters of 30–80 nm is located between the agglomerates (macropores). Macropores are permanent and can be detected by standard techniques of pore analysis, that is, adsorption–desorption of $N_2$ at 77 K. Mesopores and micropores appear in polar media able to swell the polymer. They are nonpermanent and can be detected by characterization techniques in aqueous media, such as inverse steric exclusion chromatography (ISEC) [15].

As shown in Table 1, Amberlyst 36 and DL-I/03 (medium cross-linking degree) have permanent macropores in the dry state, whereas in Amberlyst 70 and DL-H/03 (low cross-linking degree), macropores appear on swelling in polar medium. Comparing surface areas, pore volume, and mean pore diameters between dry and swollen states clearly shows that new intermediate pores (mesopores) are accessible in the presence of polar solvents in the four macroporous Amberlyst resins. In the case of gel resins CT-224 and Dowex 50W × 4, no macropores originate from the swelling by water or alcohol.

A good view of the three-dimensional polymer network of swollen polymer is given by the Ogston geometrical model [16], in which micropores are described by spaces between randomly

Table 1
Properties and structural parameters of resins in dry state and swollen in water

| | Short name | Acidity (mol/kg) | $d_p$ (μm) | $T_{max}$ (K) | % DVB | $\rho_s$[c] (g/cm$^3$) | Dry state | | | | Swollen in water (ISEC method) | | | | |
|---|---|---|---|---|---|---|---|---|---|---|---|---|---|---|---|
| | | | | | | | $S_g$[d] (m$^2$/g) | $V_g$[e] (cm$^3$/g) | $d_{pore}$[f] (nm) | $\theta$[g] (%) | $S_g$ (m$^2$/g) | $V_g$ (cm$^3$/g) | $V_{sp}$ (cm$^3$/g) | $d_{pore}$[f] (nm) | $\theta$[g] (%) |
| Nafion NR50[a] | NR50 | 0.81 | 2350 | 493 | | 2.042 | 0.35 | | | | | | | | |
| CT-224[a] | CT224 | 5.14 | 750 | 423 | Low | 1.4236 | 0.0188 | | | | | | | 1.81 | 61.2 |
| Dowex 50W × 4-50[a] | Dow50 | 4.95 | 499 | 423 | Low | 1.4259 | 0.0109 | | | | | | | 1.92 | 63.5 |
| Amberlyst DL-H/03[b] | DL-H/03 | 3.39 | 698 | 443 | Low | 1.4611 | 0.087 | | | | 283 | 0.577 | 8.2 | 0.873 | 52.8 |
| Amberlyst 70[b] | A-70 | 3.01 | 549 | 473 | Low | 1.5197 | 0.0181 | | | | 176 | 0.355 | 8.1 | 1.19 | 57.4 |
| Amberlyst DL-I/03[b] | DL-I/03 | 5.46 | 627 | 443 | Medium | 1.6191 | 19.8 | 0.17 | 34.4 | 21.6 | 153 | 0.459 | 12.0 | 0.744 | 48.7 |
| Amberlyst 36[b] | A-36 | 4.87 | 624 | 423 | Medium | 1.4494 | 28.6 | 0.21 | 34.3 | 23.2 | 147 | 0.333 | 9.1 | 0.999 | 48.2 |

[a] G = Gel type or microporous.
[b] M = macroporous.
[c] Skeletal density, measured by helium displacement.
[d] BET method ($N_2$ for $S_g \geqslant 1$ m$^2$/g; Kr for $S_g < 1$ m$^2$/g).
[e] Determined by adsorption–desorption of $N_2$ at 77 K.
[f] Assuming pore cylindrical model.
[g] $\theta$ in dry state was estimated as $100V_g/(V_g + (1/\rho_s))$ and in swollen state as $100(V_g + V_{sp} - (1/\rho_s))/(V_g + V_{sp})$, respectively.

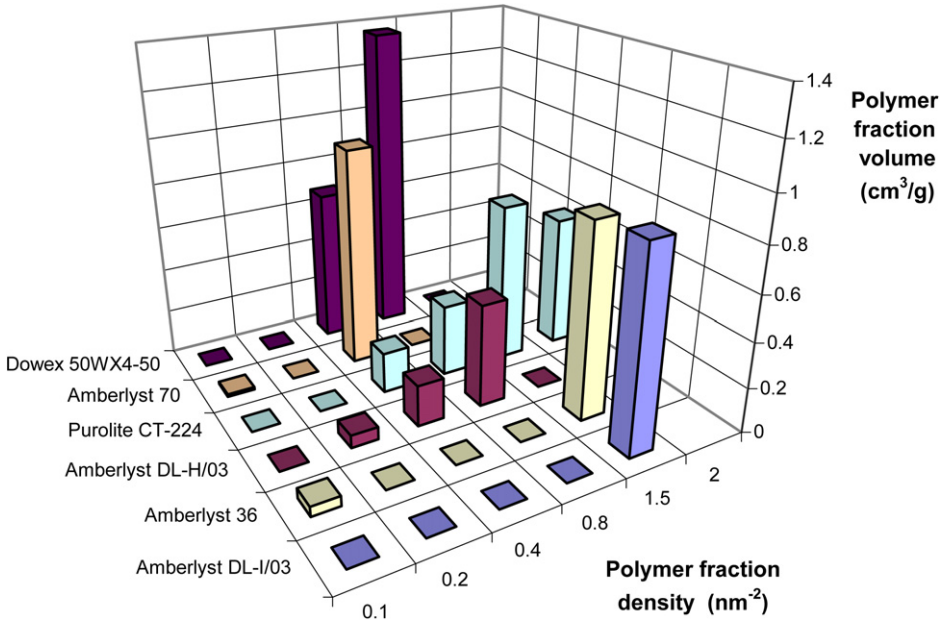


Fig. 1. ISEC pattern displayed by resins in water.

oriented rigid rods. From ISEC data, the Ogston model allows one to distinguish zones of swollen gel phase of different densities or polymer chain concentrations (total rod length per unit of volume of swollen polymer, $nm^{-2}$) and also to estimate the specific volume of swollen polymer (free space volume plus that occupied by the skeleton), $V_{sp}$. The polymer density distribution of the swollen gel phase in aqueous solution of tested S/DVB resins is shown in Fig. 1. Amberlyst 36 and DL-I/03 have polymer concentrations $\geqslant 1.5$ $nm^{-2}$, typical of a very dense polymer (poorly accessible), whereas Amberlyst 70, Amberlyst DL-H/03, CT-224, and Dowex 50W × 4 show a significant fraction of polymer density between 0.4 and 0.8 $nm^{-2}$, corresponding to a moderately expanded gel. Thus, they are far more accessible. The porosity of swollen resins considers $V_g$ (mesopores) and $V_{sp}$ (micropores) jointly. It is noteworthy that the macroporous resins, with low $V_{sp}$, have lower porosity than the gel-type resins.

NR50 is a perfluoroalkane sulfonic resin with morphology consisting of 3–5 nm clusters of $–SO_3H$-ended perfluoroalkyl ether side chains, with the clusters dispersed throughout a hydrophobic semicrystalline tetrafluoroalkyl ether matrix [17].

Physical and textural properties of H-Beta (H-BEA-25) are given in Table 2. H-Beta consists of a collection of aggregates of small crystallites ranging from 0.7 to 40 μm (mean size, about 8 μm). Crystallite size is typically in the range 0.1–0.3 μm. Acid site density was estimated by assuming one Brønsted acid site per lattice Al free of residual cations such as $Na^+$ [18]. From the $N_2$ adsorption–desorption isotherm recorded at 77 K, external surface area, $S_{ext}$, and micropore volume, $V_\mu$, were computed by the $t$-method of Lippens–de Boer [19], and pore size distribution in the mesopore and macropore range was calculated by the Barret–Joyner–Halenda method [20,21]. A more detailed report of properties of H-Beta as well as the pore distribution curve is available elsewhere [11].

Table 2
Physical and structural properties of the zeolite H-Beta

| | |
|---|---|
| Structure | H-BEA-25 |
| $SiO_2/Al_2O_3$ | 25.1 |
| Acid site concentration (mol/kg) | 1.2 |
| Mean particle size (μm) | 8.1 |
| Mean crystal size[a] (μm) | 0.1–0.3 |
| Skeletal density, $\rho_s$ ($g/cm^3$) | 2.237 |
| BET surface area, $S_g$ ($m^2/g$) | 594 |
| Pore volume, $V_g$ ($cm^3/g$) | 0.724 |
| External surface area, $S_{ext}$[b] ($m^2/g$) | 246 |
| Micropore volume, $V_\mu$[b] ($cm^3/g$) | 0.150 |
| Mesopore surface, $S_{meso}$[c] ($m^2/g$) | 232 |
| Mesopore volume, $V_{meso}$[c] ($cm^3/g$) | 0.626 |
| Mean mesopore diameter, $\bar{d}_{pore}$ (nm) | 10.8 |
| Micropore diameter[d] (nm) | 0.65 × 0.56; 0.75 × 0.57 |

[a] From SEM micrographs.
[b] Calculated by the $t$-method of Lippens–de Boer [19].
[c] Calculated according to Ref. [20].
[d] Values obtained from molecular models [21].

### 2.2. Apparatus

Experiments were carried out in a 100-ml stainless steel autoclave operated in batch mode. A magnetic drive turbine was used for mixing, and baffles were placed inside the reactor to improve agitation. Temperature was controlled to within ±1 K by an electric furnace. The pressure was set at 1.6 MPa by means of $N_2$ to maintain the reacting mixture in the liquid phase over the whole temperature range. One of the outlets was connected directly to a liquid sampling valve, which injected 0.2 μl of pressurized liquid into a gas–liquid chromatograph. More detailed information can be found elsewhere [6,22].

### 2.3. Analysis

The composition of liquid mixtures was analyzed using a split-mode operation in a HP6890A GLC apparatus equipped with a thermal conductivity detector. A 50 m × 0.2 mm × 0.5 μm methyl silicone capillary column was used to determine 1-pentanol, DNPE, water and byproducts: $C_5$ alkenes (1-pentene, 2-pentene) and branched ethers (1-(1-methylbutoxy)-pentane, 1-(2-methylbutoxy)-pentane, 2-(1-methylbutoxy)-pentane, and 2-(2-methylbutoxy)-pentane). The column was temperature-programmed with a 6-min initial hold at 318 K, followed by a 30 K/min ramp up to 453 K and holding for 5 min. Helium was used as a carrier gas at a total flow rate of 30 ml/min.

### 2.4. Procedure

Fresh catalyst and 70 ml of 1-pentanol were charged into the reactor and, after checking for leaks, heated to the desired temperature. When the reaction medium reached that temperature, the time was set as the initial instant. To monitor the concentration variation of chemicals over time, liquid samples were taken out of the reactor and analyzed hourly. Each experiment lasted 6 h. The temperature ranged from 393 to 463 K, stirring speed was set at 500 rpm, and the catalyst mass was 1 g. Before use, resins, including NR50, were dried at 390 K under vacuum for 2 h, whereas H-Beta was activated by calcination at 773 K for 3 h under air stream in a muffle furnace and kept under vacuum ($10^{-4}$ mm Hg) overnight. Catalysts were used with the commercial distribution of bead sizes.

In each experiment, 1-pentanol conversion ($X_p$), selectivity to DNPE ($S_{DNPE}$), selectivity to alkenes ($S_{alkenes}$), selectivity to branched ethers ($S_{ethers}$) and yield of DNPE with respect to 1-pentanol ($Y_{DNPE}$) were computed. $X_p$ and $S_{DNPE}$ are defined as follows:

$$X_p = \frac{\text{mole of } 1-\text{pentanol reacted}}{\text{initial mole of } 1-\text{pentanol}}, \quad (1)$$

$$S_{DNPE} = \frac{\text{mole of } 1-\text{pentanol reacted to form DNPE}}{\text{mole of } 1-\text{pentanol reacted}}. \quad (2)$$

$S_{alkenes}$ and $S_{ethers}$ are defined similarly. $Y_{DNPE}$ is defined as

$$Y_{DNPE} = \frac{\text{mole of } 1-\text{pentanol reacted to form DNPE}}{\text{initial mole of } 1-\text{pentanol}} = X_p \times S_{DNPE}. \quad (3)$$

In addition, reaction rates of DNPE formation were estimated from the experimental curve $n_{DNPE}$ versus $t$, by deriving it at time $t$ according to

$$r_{DNPE}(t) = \frac{1}{W}\left(\frac{dn_{DNPE}}{dt}\right)_t. \quad (4)$$

## 3. Results and discussion

### 3.1. Preliminary experiments

Preliminary runs were conducted on CT224, Dowex 50W × 4, and NR50 to check whether measured reaction rates were free of mass transfer effects. These were selected because CT224 and Dowex 50W × 4 were found to be the more active and NR50 was found to be the most selective among the catalysts tested in our previous work [6].

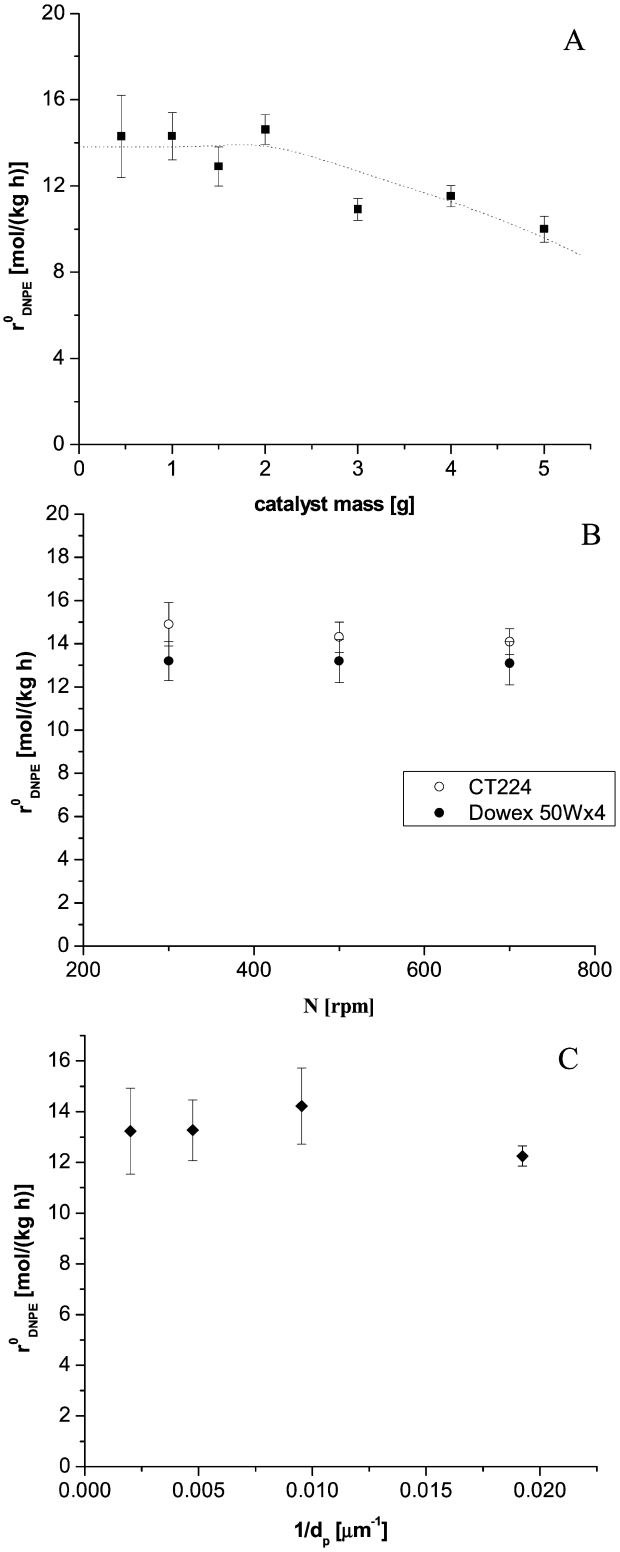


Fig. 2. Effect on initial reaction rate of (A) catalyst mass (CT-224, 423 K, 16 bar, 500 rpm), (B) stirring speed (423 K, 16 bar, 1 g of catalyst) and (C) bead size (Dowex 50W × 4, 423 K, 16 bar, 500 rpm, 1 g of catalyst).

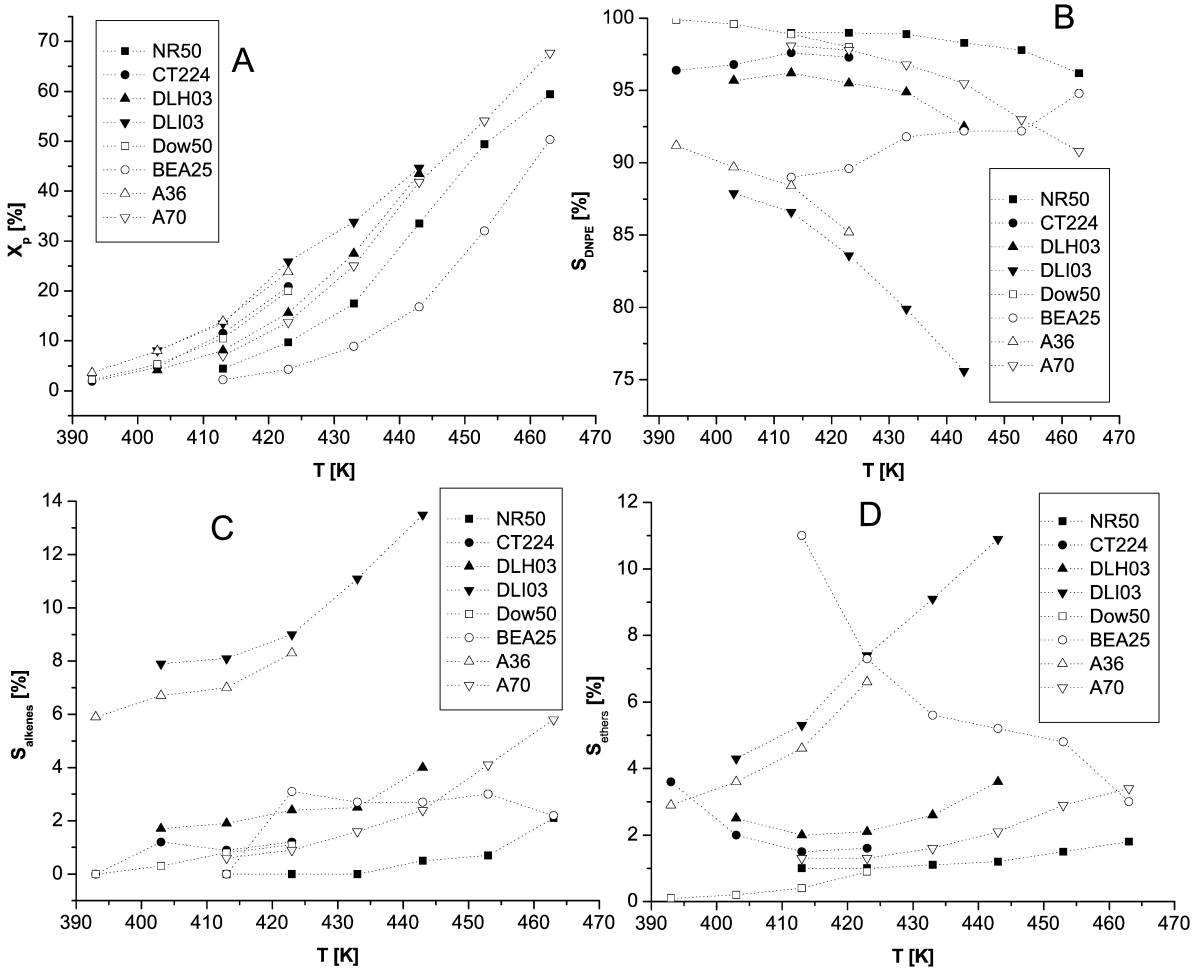


Fig. 3. 1-pentanol conversion (A), selectivity to DNPE (B), olefins (C) and branched ethers (D) as a function of temperature (16 bar, 500 rpm and 1 g catalyst).

First, the effect of the amount of catalyst was checked at 423 K with CT224. The mass of dried catalyst was changed from 0.5 to 5 g. Fig. 2A shows that for catalyst mass $\leqslant$2 g (catalyst loading $\leqslant$3.5%), the initial reaction rate was independent of the catalyst mass within the limits of experimental error, but with catalyst mass $\geqslant$2 g, the initial reaction rate decreased with increasing catalyst mass. Therefore, using $>$2 g of catalyst was a source of inaccuracy in the calculations, so that henceforth runs were performed on 1 g of catalyst.

Then the influence of external mass transfer was tested at 423 K on Dowex 50W $\times$ 4 and CT-224 in a series of experiments with stirring speeds of 50–700 rpm. As shown in Fig. 2B, initial reaction rates were the same between 300 and 700 rpm within the limits of experimental error. External mass transfer influence was also tested on NR50, because its beads are far larger than those of both resins. It was found that estimates of reaction rate at 443 K were the same, within the limits of experimental error, in the range 100–900 rpm [22]. As a result, stirring speed was set at 500 rpm for all of the catalysts.

Finally, to assess the influence of catalyst size on the reaction rate, experimental runs on Dowex 50W $\times$ 4 batches of 400, 200, 100, and 50 mesh (particle diameter, $d_p$, of 0.05–0.5 mm) were performed at 423 K and 500 rpm. As shown in Fig. 2C, initial reaction rates do not depend on the particle size within the limits of experimental error. This is because resin beads swell sufficiently in aqueous medium, allowing good accessibility to the inner active centers. Nevertheless, diffusion influence cannot be excluded a priori above 423 K in thermally stable resins in spite of the fact that, on the basis of ISEC data, we can assume ready accessibility to sulfonic groups of the resin gel phase. For NR50, the influence of catalyst size was tested by comparing reaction rates measured on NR50 beads and on a 0.2-mm-thick perfluorinated membrane with the same number of acid groups (Nafion 117). It was found that reaction rates were the same within $\pm$2% [23]. As for H-Beta, the influence of diffusion is reduced to negligible proportions with crystals smaller than 100 μm [11].

### 3.2. 1-Pentanol conversion, selectivity to DNPE and byproducts, and DNPE yield

Catalysts were tested at 393–463 K and 500 rpm using 1 g of dried commercial beads of solid, as stated above. The working temperature range was selected by considering the maximum operating temperature of each resin. Fig. 3 shows 1-pentanol conversion and selectivity to DNPE and byproducts at 6 h of reaction time. $X_p$ increased with temperature, as was expected

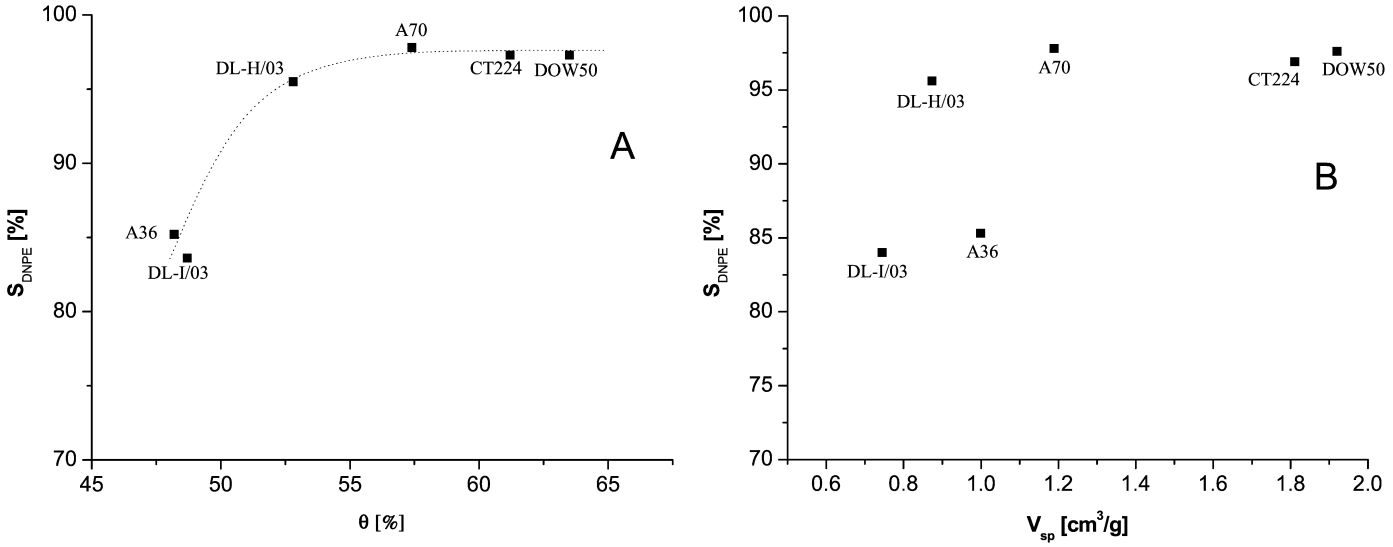


Fig. 4. Selectivity to DNPE at 423 K as a function of $\theta$ (A) and $V_{sp}$ (B) of swollen resins.

Table 3
Values of Hammett acidity function ($-H_0$) of some catalysts [26]

| Catalyst | Aqueous conditions | Nonaqueous conditions |
|---|---|---|
| $H_2SO_4$ (100%) | 12 | 12 |
| $H_2SO_4$ (86%)[b] | 8.5 | 8.5 |
| $H_2SO_4$ (70%) | 5.9 | 5.9 |
| $H_2SO_4$ (63%) | 4.9 | 4.9 |
| $H_2SO_4$ (48%) | 2.66 | 2.66 |
| $H_2SO_4$ (35%) | 2.16 | 2.16 |
| Nafion NR50[b] | 8.4 | |
| Amberlyst 35[a] | 2.65 | 5.6 |
| Amberlyst 15[a] | 2.2 | |
| Zeolite HZSM-5 | | 5.7 |
| Zeolite HY | | 4.4 |
| Zeolite H-Beta[c] | | $4.4 < -H_0 < 5.7$ |

[a] Amberlyst 15 is assumed to be representative of conventionally sulfonated resins (a $SO_3H$ group per benzene ring), whereas Amberlyst 35 does of oversulfonated ones [K.D. Topp, personal communication].
[b] Farcasiu et al. [27].
[c] Beck and Haw [28].

far from chemical equilibrium, and $S_{DNPE}$ decreased for all catalysts but H-Beta, which shows an opposite selectivity pattern.

As a rule, the higher the acidity and acid strength of catalysts, the higher the $X_p$. At the same temperature, $X_p$ decreased in the following order: S/DVB resins, NR50, and H-Beta. Among the resins, below 423 K, Amberlyst 36, DL-I/03, and CT-224 (oversulfonated) were more active than Dowex 50W × 4, Amberlyst 70, and DL-H/03. The former three exhibited greater acid capacity and acid strength than the latter three (see Tables 1 and 3). Also, at 443 K, Amberlyst DL-I/03 was slightly more active than Amberlyst 70 and DL-H/03. Finally, even at 463 K, Amberlyst 70 was more active than NR50 and H-Beta, mainly because of its greater capacity. NR50 was more active than H-Beta due to its higher acid strength.

$S_{DNPE}$ decreased with temperature due to the formation of alkenes and, consequently, branched ethers. The amounts of alkenes and branched ethers were generally quite similar, whereas $C_5$ alcohols were not detected. This suggests that branched ethers are formed by the reaction between an alkene and the appropriate alcohol. Dowex 50W × 4 at 393–413 K and NR50 423–463 K were the most selective to DNPE.

Fig. 4 shows that at 423 K, $S_{DNPE}$ on S/DVB resins increased with $V_{sp}$ and porosity, reaching a maximum of 98% for Dowex 50W × 4, CT-224, and Amberlyst 70. From the two plots, it can be seen that good selectivity was obtained with catalysts showing a large swollen volume and an accessible gel phase. Amberlyst 70, DL-H/03, CT-224, and Dowex 50W × 4 (swollen polymer densities in the range 0.4–1.5 nm$^{-2}$) were more selective than Amberlyst 36 and DL-I/03 (polymer densities of 1.5–2 nm$^{-2}$). Therefore, the first have a much more flexible polymer network and, assuming that reaction takes place mainly in the gel phase, can better accommodate the reaction intermediate and be more selective.

The mechanism of 1-pentanol dehydration to ether depends on the water content of the reaction medium [24]. In excess of water, the reaction mechanism could involve the in situ formation of an oxonium ion, which is a good leaving group, by protonation (specific acid catalysis). The ether is formed by the nucleophilic attack of alcohol on the oxonium ion in a $S_N2$ bimolecular reaction [25]. Dehydration to pentenes occurs through a monomolecular reaction of elimination ($E_1$ type). However, when there is no water in the system or alcohol is in excess, the reaction could take place by the initial reaction of 1-pentanol at –$SO_3H$ sites to form 1-pentylsulfate (general acid catalysis) [R. Banavali, personal communication]. The ether would be formed by the attack of a second alcohol molecule on the sulfate in a $S_N2$ reaction. Whatever the reaction mechanism, the $S_N2$ reaction is greatly limited by steric hindrance on rigid polymers, and the occurrence of $E_1$ increases, leading to increased $S_{alkenes}$ and $S_{ethers}$ ethers.

Selectivity is also influenced by the acid strength of S/DVB sulfonated copolymers. Resins with higher acid strength more readily catalyzes the dehydration to olefin so that $S_{DNPE}$ decreases, as shown by the data for Amberlyst 36 and Amberlyst DL/I-03.

Table 4
DNPE yields (%) at 6 h of reaction (1 g catalyst, 500 rpm)

| $T$ (K) | NR50 | H-BEA 25 | CT224 | DL-H/03 | DL-I/03 | Dow50 | A-36 | A-70 |
|---|---|---|---|---|---|---|---|---|
| 393 | | | 1.8 | | | 2.2 | 3.3 | |
| 403 | | | 4.6 | 3.9 | 7.1 | 5.2 | 7.2 | |
| 413 | 4.4 | 2.0 | 11.2 | 7.7 | 11.7 | 10.4 | 12.3 | 6.9 |
| 423 | 9.6 | 3.8 | 20.3 | 14.9 | 21.7 | 19.6 | 20.2 | 13.4 |
| 433 | 17.3 | 8.1 | | 26.1 | 27.0 | | | 24.3 |
| 443 | 32.9 | 15.5 | | 40.2 | 33.8 | | | 39.9 |
| 453 | 48.3 | 29.5 | | | | | | 50.3 |
| 463 | 57.1 | 47.7 | | | | | | 61.4 |

DNPE yields are given in Table 4. $Y_{DNPE}$, just like $X_p$, increased with temperature, with the higher values corresponding to Amberlyst 70, NR50, and H-Beta (in decreasing order) at 463 K. Therefore, Amberlyst 70 appears to be the best option below 463 K, because it showed the highest $X_p$ and $Y_{DNPE}$, with a $S_{DNPE} \geqslant 93\%$ at 463 K. NR50, which is the most selective, has the drawbacks of low acid capacity and surface area. Despite this, its activity increased remarkably with increasing temperature. As for H-Beta, $S_{DNPE}$ increased with temperature, in contrast to what is observed with S/DVB resins, and was >96% at 463 K, suggesting that H-Beta could be a good option for catalyzing the dehydration of 1-pentanol to DNPE at temperatures above 463 K.

### 3.3. Initial reaction rates

Table 5 shows initial reaction rates, $r^0_{DNPE}$, at working temperatures. As was expected, $r^0_{DNPE}$ strongly increased with temperature. At the same temperature (i.e., 423 K), the greater the acid capacity, the higher the reaction rate. Thus, S/DVB resins Amberlyst 36, DL-I/03 and CT224 showed the highest $r^0_{DNPE}$ values. However, $r^0_{DNPE}$ on NR50 was much higher than expected based on its acid capacity. This fact is usually explained by the higher acid strength of $-SO_3H$ groups in Nafion resins with respect to S/DVB catalysts (Table 3) due to the electronegativity of F atoms of the NR50 skeleton [26,27]. To assess the effect of the acid strength of catalysts on DNPE synthesis, initial rates per $-SO_3H$ group, $r^0_{DNPE,eq}$ (turnover numbers) were computed. As shown in Table 5, the $r^0_{DNPE,eq}$ of NR50 was two to three times that of S/DVB resins due to its higher acid strength. Moreover, oversulfonated S/DVB resins had slightly higher $r^0_{DNPE,eq}$ than the other resins.

Among the catalysts tested, H-Beta showed the lowest $r^0_{DNPE}$ and $r^0_{DNPE,eq}$. This can be explained by the fact that DNPE synthesis proceeds primarily on the external surface, which is 40% of total surface area [9–11]. Moreover, the amount of active centers is only 25% of those of conventional resins. As a result, the surface density of acid sites is low compared with that of resins. In this way, the formation of the reaction intermediate could be hindered by the low surface concentration of $H^+$, as demonstrated by the low turnover number of the zeolite, despite the fact that the acid strength of H-Beta is similar to that of ion exchangers (see Table 3) [26,28].

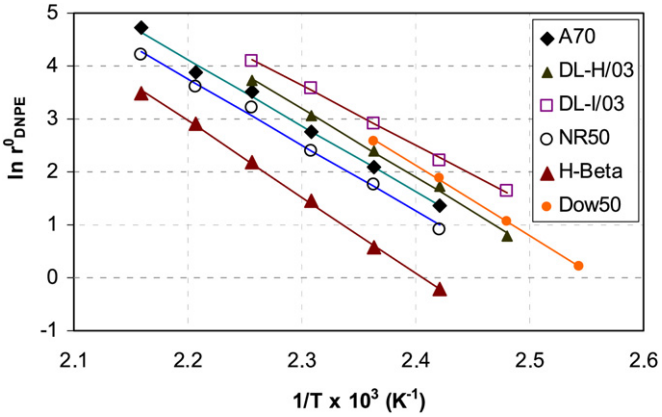


Fig. 5. Arrhenius plot of initial reaction rates for some tested catalysts.

### 3.4. Kinetic studies

Preliminary experiments show that diffusion does not affect the reaction rate on ion-exchange resins at temperatures below 423 K. On the other hand, Arrhenius plots of initial reaction rates for thermally stable resins are good straight lines (Fig. 5). Thus, there are no diffusion concerns in the entire temperature range studied on the resins or NR50. Because external mass transfer does not affect reaction rate either, kinetic studies of the reaction over each catalyst were undertaken. Reaction rates were estimated by Eq. (4) from experiments outlined in Section 3.2. Because the reaction mixture is nonideal, rate equations are given in terms of 1-pentanol, DNPE, and water activities. Activity coefficients were computed using the UNIFAC-DORTMUND predictive method [29].

The kinetic model considered in this work is based on the most commonly quoted mechanism in the literature for dehydration of alcohols to ether on acidic resins: Langmuir–Hinshelwood–Hougen–Watson (LHHW) and its derived form, Eley–Rideal (ER). Considering the adsorption-reaction–desorption process, we can assume that the best kinetic model could stem from a LHHW mechanism wherein two 1-pentanol molecules adsorbed each on a single center react to give DNPE and water adsorbed on a single center. On the basis of the more recent work on CT-224 [30,31], no additional sites were considered to take part in the surface reaction step. Assuming that the rate-limiting step is surface reaction, the LHHW formalism leads to the following kinetic model:

$$r_{DNPE} = \frac{\hat{k} K_P^2 (a_P^2 - a_D a_W / K)}{(1 + K_P a_P + K_D a_D + K_W a_W)^2}. \quad (5)$$

The analogous ER mechanism assumes that a 1-pentanol molecule from solution reacts with an adsorbed 1-pentanol molecule, with the ether adsorbed on the surface. If surface reaction is considered the rate-limiting step, then a similar equation is obtained:

$$r_{DNPE} = \frac{\hat{k} K_P (a_P^2 - a_D a_W / K)}{1 + K_P a_P + K_D a_D}. \quad (6)$$

A second ER mechanism in which water remains adsorbed into the catalyst surface was considered. In this case, the following

Table 5
Initial reaction rate and initial turnover number

| Catalyst | $r^0_{DNPE}$ (mol/(h kg)) | | | | | | | | $r^0_{DNPE,eq}$ (mol/(h eq $H^+$)) | | | | | | | |
|---|---|---|---|---|---|---|---|---|---|---|---|---|---|---|---|---|
| | 393 K | 403 K | 413 K | 423 K | 433 K | 443 K | 453 K | 463 K | 393 K | 403 K | 413 K | 423 K | 433 K | 443 K | 453 K | 463 K |
| NR50 | | | 2.5 | 5.8 | 10.9 | 24.8 | 36.8 | 67.3 | | | 2.8 | 6.5 | 12.2 | 27.8 | 41.3 | 75.6 |
| HBEA25 | | | 0.8 | 1.8 | 4.3 | 8.8 | 18.2 | 32.7 | | | 0.6 | 1.5 | 3.6 | 7.4 | 15.2 | 27.3 |
| CT224 | 1.0 | 2.5 | 7.3 | 15.7 | | | | | 0.2 | 0.5 | 1.4 | 3.1 | | | | |
| DL-H/03 | | 2.2 | 5.6 | 11.0 | 21.4 | 41.9 | | | | 0.6 | 1.7 | 3.2 | 6.3 | 12.4 | | |
| DL-I/03 | | 5.2 | 9.3 | 18.4 | 36.1 | 60.2 | | | | 1.0 | 1.7 | 3.4 | 6.6 | 11.0 | | |
| Dow50 | 1.2 | 2.9 | 6.5 | 13.2 | | | | | 0.3 | 0.6 | 1.3 | 2.7 | | | | |
| A-36 | 1.8 | 4.5 | 9.1 | 18.9 | | | | | 0.4 | 0.9 | 1.9 | 3.9 | | | | |
| A-70 | | | 3.9 | 8.1 | 15.6 | 33.6 | 48.7 | 112 | | | 1.3 | 2.7 | 5.2 | 11.2 | 16.2 | 37.3 |

rate equation is obtained:

$$r_{DNPE} = \frac{\hat{k}K_P(a_P^2 - a_D a_W/K)}{1 + K_P a_P + K_W a_W}. \quad (7)$$

Some preliminary long-time experiments (>48–72 h) showed that equilibrium conversions are >90% in the whole working temperature range. Because only in a few experiments did $X_p$ exceed 40%, it was assumed that the influence of reverse reaction on the global rate was low, and some discrepancies could be expected only at high temperatures in the kinetic model-fitting procedure. Thus, Eqs. (5)–(7) reduce to

$$r_{DNPE} = \frac{\hat{k}K_P^2 a_P^2}{(1 + K_P a_P + K_D a_D + K_W a_W)^2}, \quad (8)$$

$$r_{DNPE} = \frac{\hat{k}K_P a_P^2}{1 + K_P a_P + K_D a_D}, \quad (9)$$

and

$$r_{DNPE} = \frac{\hat{k}K_P a_P^2}{1 + K_P a_P + K_W a_W}. \quad (10)$$

Equations (8)–(10), and simplified equations obtained by assuming negligible adsorption of alcohol, ether, and/or water and/or a negligible amount of free active sites, were fitted to find the one that best represents the rate data. For all catalysts, the best model from a statistical standpoint (minimum sum of squares, random residuals, and low parameter correlation) with physicochemical meaning (positive activation energy and negative adsorption enthalpies and entropies) appeared to be

$$r_{DNPE} = \frac{\hat{k}a_P^2}{a_P + (K_D/K_P)a_D}, \quad (11)$$

where the adsorption equilibrium constants $K_P$ and $K_D$ are grouped for fitting purposes. The temperature dependence of rate constant, $\hat{k}$, and $K_P/K_D$ are

$$\hat{k} = \exp(b_1)\exp\left[-b_2\left(\frac{1}{T} - \frac{1}{\bar{T}}\right)\right] \quad (12)$$

and

$$K_D/K_P = \exp(b_3)\exp\left[-b_4\left(\frac{1}{T} - \frac{1}{\bar{T}}\right)\right]. \quad (13)$$

The subtraction of the mean experimental temperature was included to minimize the correlation between fitted parameters, namely the $b$'s. Their standard error was estimated by the jackknife method [32].

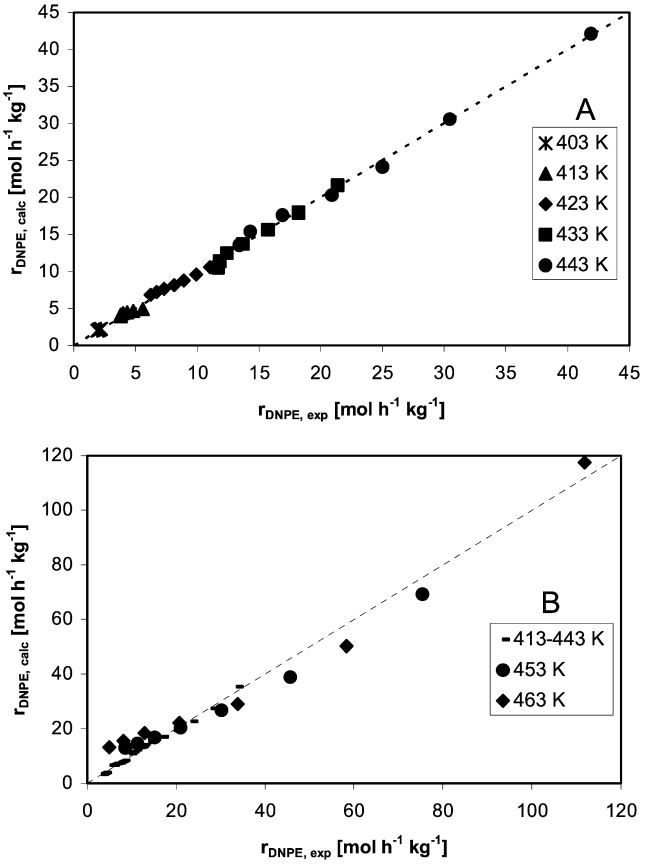


Fig. 6. Estimated vs experimental reaction rate at all temperatures for (A) Amberlyst DL-H/03 and (B) Amberlyst 70.

Plots of calculated by Eq. (11) versus experimental rates (for example, Fig. 6A for Amberlyst DL-H/03), show that the fit is satisfactory. However, at 453 and 463 K, some deviations are seen (for example, Fig. 6B for Amberlyst 70). At such temperatures, the rate model should be upgraded, possibly by considering the reverse reaction.

Equation (11) stems from the ER mechanism wherein the ether formed remains adsorbed on the surface; the number of free active centers being negligible, what is feasible for liquid-phase reactions. Because water adsorbs preferably on $SO_3H$ groups, due to the possibility of forming up to four hydrogen bonds with sulfonic groups, it is possible that water occupies

Table 6
Activation energy and adsorption enthalpy and entropy difference between DNPE and alcohol

| Catalyst | $E_a$ (kJ/mol) | $\Delta H_D - \Delta H_P$ (kJ/mol) | $\Delta S_D - \Delta S_P$ (kJ/mol K) |
|---|---|---|---|
| NR50 | 109.3 ± 3.4 | 184 ± 44 | 0.40 ± 0.12 |
| HBEA25 | 121.2 ± 1.7 | 150 ± 100 | 0.32 ± 0.28 |
| CT224 | 119.1 ± 4.3 | −140 ± 45 | −0.34 ± 0.11 |
| DL-H/03 | 110.6 ± 2.6 | 7.7 ± 14 | 0.024 ± 0.038 |
| DL-I/03 | 113.4 ± 6.5 | 53 ± 22 | 0.139 ± 0.056 |
| Dow50 | 114.7 ± 1.5 | 272 ± 56 | 0.65 ± 0.14 |
| A-36 | 110.1 ± 2.1 | 9.2 ± 11 | 0.037 ± 0.029 |
| A-70 | 114.7 ± 5.4 | 63 ± 28 | 0.146 ± 0.076 |

Table 7
Activation energy value for CT-224 quoted in literature

| $E_a$ (kJ/mol) | Ref. |
|---|---|
| 146 ± 4 | [30] |
| 128.3 ± 4.4 | This work[a] |
| 119.1 ± 4.3 | This work |
| 115 ± 6 | [31] |
| 99 ± 8 | [6][a] |

[a] From Arrhenius plot of initial reaction rates.

a large, but almost constant, amount of active sites, preventing them from catalyzing the reaction. However, ascertaining this point requires further work.

Activation energies were obtained from the temperature dependence of $\hat{k}$, seeing that $b_2 = E_a/R$ [Eq. (12)]. As shown in Table 6, they range from 110 to 120 kJ/mol, so that temperature dependence is of the same order on each catalyst, as Fig. 5 also shows. Only $E_a$ values for CT-224 were found in the open literature (see Table 7). The values reported here are in the middle of the quoted range. It is to be noted that the value 146 ± 4 kJ/mol reported in [30] is probably influenced by the short range of alcohol and ether activities explored in that work. Moreover, the lowest (100 ± 8 kJ/mol) can be explained by the fact that the used catalyst mass was excessively high [6].

Parameters $b_4$ and $b_3$ of Eq. (13) supply information on the difference between adsorption enthalpies and entropies of ether and alcohol, respectively. Table 6 shows the estimates of $\Delta H_D - \Delta H_P$ and $\Delta S_D - \Delta S_P$. These values indicate that DNPE adsorption is stronger than that of 1-pentanol but in the case of CT-224. However, the high standard error associated with $b_3$ and $b_4$ estimates suggest that adsorption of ether is less significant than that of 1-pentanol, which could imply little sensitivity to such parameters in the fitting procedure.

## 4. Conclusion

The thermally stable resin Amberlyst 70 appears to be the best choice for the dehydration of 1-pentanol to DNPE among the catalysts tested. Compared with the other S/DVB resins, its thermal stability led to higher conversion and yield, with good selectivity, even at 463 K. Nafion NR50 was the most selective at all temperatures, but its activity was lower than that of Amberlyst 70 due to the low concentration of sulfonic groups in the polymer matrix. H-Beta zeolite was the least active of the catalysts tested. A kinetic model based on an ER mechanism in which the surface reaction between adsorbed 1-pentanol and an alcohol molecule from the liquid phase was the rate-limiting step satisfactorily describes the rate data. Activation energies were between 110 and 120 kJ/mol for each catalyst.

## Acknowledgments

Financial support was provided by the State Education, Universities, Research & Development Office of Spain (project PPQ2000-0467-P4-02). The authors thank Dr. Karel Jerabek (Institute of Chemical Process Fundamentals, Prague) for ISEC structural and textural analysis and Drs. Rajiv Banavali and Klaus Dieter Topp (Rohm and Haas Co.) for their helpful comments. They also thank Rohm and Haas for providing some ion-exchange resins, including thermally stable copolymers.

## Appendix A. Nomenclature

| | |
|---|---|
| $a_j$ | activity of compound $j$ |
| $d_p$ | particle diameter (μm) |
| $d_{pore}$ | pore diameter (nm) |
| $E_a$ | activation energy (kJ/mol) |
| $\Delta H_j$ | adsorption enthalpy of compound $j$ (kJ/mol) |
| $-H_0$ | Hammet activity function |
| $\hat{k}$ | intrinsic rate constant (mol h$^{-1}$ g$^{-1}$) |
| $K_j$ | adsorption equilibrium constant of $j$ |
| $K$ | thermodynamic equilibrium constant |
| $n_{DNPE}$ | number DNPE moles |
| $N$ | stirring speed (rpm) |
| $r_{DNPE}$ | reaction rate of DNPE synthesis (mol h$^{-1}$ kg$^{-1}$) |
| $r^0_{DNPE}$ | initial reaction rate of DNPE synthesis (mol h$^{-1}$ kg$^{-1}$) |
| $r^0_{DNPE,eq}$ | initial reaction rate of DNPE synthesis per sulfonic group (mol h$^{-1}$ kg$^{-1}$) |
| $R$ | gas constant (J mol$^{-1}$ K$^{-1}$) |
| $\Delta S_j$ | adsorption entropy of compound $j$ (J mol$^{-1}$K$^{-1}$) |
| $S_{DNPE}$ | selectivity to DNPE (%) |
| $S_{ext}$ | external surface area of zeolite H-Beta (m$^2$ g$^{-1}$) |
| $S_g$ | surface area (m$^2$ g$^{-1}$) |
| $S_{meso}$ | surface area of meso- and macropores in H-Beta (m$^2$ g$^{-1}$) |
| $t$ | time (h) |
| $T$ | temperature (K) |
| $T_{max}$ | maximum operating temperature (K) |
| $V_g$ | pore volume (cm$^3$ g$^{-1}$) |
| $V_{meso}$ | pore volume relative to meso- and macropores in H-Beta (cm$^3$ g$^{-1}$) |
| $V_{sp}$ | specific volume of the swollen polymer phase (cm$^3$ g$^{-1}$) |
| $V_\mu$ | pore volume relative to micropores of zeolite H-Beta (cm$^3$ g$^{-1}$) |
| $W$ | weight of dry catalyst (g) |
| $X_p$ | conversion of 1-pentanol (%) |
| $Y_{DNPE}$ | DNPE yield |

*Greek letters*

| | |
|---|---|
| $\rho_s$ | skeletal density (g/cm$^3$) |
| $\theta$ | porosity |

*Subscripts*

| | |
|---|---|
| D | DNPE, di-*n*-pentyl ether |
| P | 1-pentanol |
| W | water |

## References


[1] A. Douaud, Hydrocarbon Proc. 74 (2) (1995) 55.
[2] G.C. Pecci, M.G. Clerici, M.G. Giavazzi, F. Ancillotti, M. Marchionna, R. Patrini, IX International Symposium on Alcohol Fuels, vol. 1, 1991, p. 321.
[3] F. Giavazzi, D. Terna, D. Patrini, F. Ancillotti, G.C. Pecci, R. Trerè, M. Benelli, IX International Symposium on Alcohol Fuels, vol. 1, 1991, p. 327.
[4] J. Van Heerden, J.J. Botha, P.N.J. Roets, XII International Symposium on Alcohol Fuels, vol. 1, Tsinghua Univ. Press, Beijing, 1998, p. 188.
[5] R. Patrini, M. Marchionna, UK Patent Application GB 2.323.844 A, 1998.
[6] J. Tejero, F. Cunill, M. Iborra, J.F. Izquierdo, C. Fité, J. Mol. Catal. A Chem. 182–183 (2002) 541.
[7] J.R. Collin, D. Ramprasad, European Patent Application EP 1 479 665 (2004).
[8] F. Collignon, M. Mariani, S. Moreno, M. Remy, G. Poncelet, J. Catal. 166 (1997) 53.
[9] F. Collignon, G. Poncelet, J. Catal. 202 (2001) 68.
[10] F. Collignon, R. Loenders, J.A. Martens, P.A. Jacobs, G. Poncelet, J. Catal. 182 (1999) 302.
[11] M. Iborra, J. Tejero, C. Fité, F. Cunill, J.F. Izquierdo, J. Catal. 231 (2005) 77.
[12] A.A. Nikolopoulos, A. Kogelbauer, J.G. Goodwin Jr., G. Marcelin, Appl. Catal. 119 (1994) 69.
[13] S. Fisher, R. Kunin, Anal. Chem. 27 (1955) 1191.
[14] A. Guyot, in: D.C. Sherrington, P. Hodge (Eds.), Syntheses and Separations Using Polymers Supports, Wiley, Chichester, 1988, p. 15, chapt. 1.
[15] K. Jerabek, ACS Symp. Ser. 635 (1996) 211.
[16] A.G. Ogston, Trans. Faraday Soc. 54 (1958) 1754.
[17] Q. Deng, Y. Hu, R.B. Moore, C.L. McCormick, K.A. Mauritz, Chem. Mater. 9 (1997) 36.
[18] M.A. Ali, B.J. Brisdon, W.J. Thomas, Appl. Catal. 197 (2000) 303.
[19] M.J. Remy, G.A. Poncelet, J. Phys. Chem. 99 (1995) 773.
[20] E.P. Barret, L.G. Joyner, P.P. Halenda, J. Am. Chem. Soc. 73 (1951) 373.
[21] R. Szostack, in: Handbook of Molecular Sieves, Van Nostrand–Reinhold, New York, 1992, p. 93.
[22] R. Bringué, MS Chem. Eng. thesis, University of Barcelona, 2004.
[23] O. Ordeig, MS Chem. Eng. thesis, University of Barcelona, 2003.
[24] B.C. Gates, W. Rodriguez, J. Catal. 31 (1973) 27.
[25] G.A. Olah, T. Shamma, G.K. Surya Prakash, Catal. Lett. 46 (1997) 1.
[26] E.G. Lundquist, K. Beshah, in: 213th ACS National Meeting, San Francisco, 2003.
[27] D. Farcasiu, A. Ghenciu, G. Marino, K.D. Rose, J. Am. Chem. Soc. 119 (1997) 11826.
[28] J.W. Beck, J.F. Haw, J. Phys. Chem. 99 (1995) 1076.
[29] R. Wittig, J. Lohmann, Ind. Eng. Chem. Res. 42 (2003) 183.
[30] F. Cunill, J. Tejero, C. Fité, M. Iborra, J.F. Izquierdo, Ind. Eng. Chem. Res. 44 (2005) 318.
[31] J. Tejero, C. Fité, M. Iborra, J.F. Izquierdo, R. Bringué, F. Cunill, Appl. Catal. 308 (2006) 223.
[32] M.S. Caceci, Anal. Chem. 61 (1989) 2324.